Paraglacial gravitational deformations in the SW Alps: a review of field investigations, ^{10}Be cosmogenic dating and physical modelling

S. El Bedoui, T. Bois, H. Jomard, et al.

Geological Society, London, Special Publications 2011; v. 351; p. 11-25
doi: 10.1144/SP351.2

Paraglacial gravitational deformations in the SW Alps: a review of field investigations, ^{10}Be cosmogenic dating and physical modelling

S. EL BEDOUI[1], T. BOIS[2]*, H. JOMARD[3], G. SANCHEZ[4], T. LEBOURG[2], E. TRICS[2], Y. GUGLIELMI[5], S. BOUISSOU[2], A. CHEMENDA[2], Y. ROLLAND[4], M. CORSINI[4] & J. L. PÉREZ[6]

[1]*LRPC Nancy, 71 rue de la Grande Haie, 54510 Tomblaine, France*

[2]*GEOAZUR CNRS-UNS-IRD-UPMC, UMR 6526, Nice Sophia-Antipolis University, 250 Avenue de Albert Einstein, 06560 Sophia-Antipolis, France*

[3]*Institute of Radioprotection and Nuclear Safety (IRSN), Fontaine-aux-Roses, France*

[4]*GEOAZUR CNRS-UNS-IRD-UPMC, UMR 6526, Nice Sophia-Antipolis University, Avenue de Valrose, 06000 Nice, France*

[5]*Centre de Sédimentologie–Paléontologie, Université de Provence Aix-Marseille 1, 3 Place Victor Hugo, 13331 Marseille Cedex 03, France*

[6]*Centre des Etudes Techniques de l'Equipement Méditerranée, 52 Bd Stalingrad, 06520 Nice, France*

**Corresponding author (e-mail: bois@geoazur.unice.fr)*

Abstract: Catastrophic deep-seated landslides (DSL) are generally considered to be the result of large slope deformations also known as deep-seated gravitational slope deformation (DSGSD). This paper aims to build a synthesis of multiple studies made in the Tinée Valley (southern French Alps) to assess the geometrical, kinematical, mechanical and chronological relationships between these two gravitational processes.

At the scale of the valley, data issued from geological, geomorphological and ^{10}Be dating indicate a clear geometrical link between DSGSD and DSL occurring at the base of the slope and suggest that gravitational slope evolution began after the glacial retreat (13 ka BP). This is supported by the example of the well-documented La Clapière slope. A continuous evolution process is characterized geometrically and temporally from geomorphic observations and analogue modelling. Coupling structural, geomorphological, physical and chronological studies allowed us to propose a four-dimensional (4D) deformation model mechanically correlated with progressive failure concept. The validity and variability of this reference site are discussed at the valley scale (taking Isola and Le Pra slope deformation as examples).

It allows a rough estimation of the state of slope deformation at the valley scale to be constructed and the slope evolution with time to be considered. This 4D model could then be considered as a reference for other deep-seated gravitational slope deformations in comparable Alpine valleys.

Gravitational slope deformation plays an important role in relief evolution of mountain ranges (Jarman 2006); however, the interconnected processes leading from large spatial and timescale deep-seated gravitational slope deformation (DSGSD) (Dramis & Sorriso-Valvo 1994) to catastrophic rock slope failure remain poorly understood (Agliardi *et al.* 2001; Ballantyne 2002).

Glacier retreat in Alpine valleys is often considered to be a major conditioning factor in slope destabilization (Evans & Clague 1994; Ballantyne 2002; Tibaldi *et al.* 2004; Bigot-Cormier *et al.* 2005; Hippolyte *et al.* 2006; Apuani *et al.* 2007). The main deglaciation effects on gravitational motion include topographic change of valleys (Savage & Varnes 1987; Augustinus 1995) and/or debuttressing of slopes leading to tensile stress state (Hutchinson 1988; Apuani *et al.* 2007). Both effects could strongly influence *in situ* stress conditions and rock strength parameters at the slope scale (Bachmann 2006).

Structural heterogeneities, such as inherited tectonic faults and fractures, are also assumed to play a dominant role in gravitational slope failure

From: JABOYEDOFF, M. (ed.) *Slope Tectonics*. Geological Society, London, Special Publications, **351**, 11–25.
DOI: 10.1144/SP351.2 0305-8719/11/$15.00

processes (Scavia 1995; Kaneko *et al.* 1997; Hermanns & Strecker 1999; Bachmann *et al.* 2004; Brideau *et al.* 2005; Jomard 2006; Bois *et al.* 2008). It is also commonly admitted that progressive failure within a rock slope can initiate and propagate through preferential weakened fault zones (Sartori *et al.* 2003; Bachmann *et al.* 2004; Willenberg 2004).

This paper focuses on a post-glacial Alpine area: the Tinée Valley (southern French Alps), which was affected by consecutive glaciations during the Quaternary period. Slopes located in this area are affected by recent DSGSD and deep-seated landslides (DSL) (Follacci 1987; Julian & Anthony 1996; Jomard 2006). This review paper is the synthesis of different approaches: field investigations, cosmonuclide dating of gravitational events and physical modelling that were performed at the valley scale and at the slope scale (the La Clapière slope) in order to: (i) establish chronological and physical links between DSGSD and DSL; and (ii) propose a model of slope deformations including some geomechanical considerations.

To this end, the La Clapière slope is described in this paper as an observatory site used to understand the slope deformation evolution processes linking DSGSD and catastrophic rock collapses.

Regional-scale gravitational deformation in the upper Tinée Valley

General settings

The Argentera–Mercantour massif is the southernmost external crystalline massif of the Western Alps. It is characterized by a polyphased deformation evolution from Variscan to Alpine orogenies (Corsini *et al.* 2004). The basement consists of high-grade metamorphic and intrusive rocks of late Carboniferous age (Ferrara & Malaroda 1969). It is unconformably covered by a marine sedimentary succession of Late Carboniferous–Cenozoic age, partly detached at the level of the Triassic evaporites (Faure-Muret 1955) and overthrusted by Penninic clastic units during the Late Eocene–Early Oligocene (Autapie nappe and Parpaillon nappe) (Tricart 1984). The upper Tinée Valley represents the western boundary between the basement with its Permo-Triassic tegument and the detached Mesozoic sedimentary cover (Figs 1 & 2). The basement rocks are migmatitic paragneisses with meta-granodioritic intrusions (Faure-Muret 1955). Ductile fabrics present a global N130° dipping to the NE foliation. The main slope directions are collinear to the major N110°–140° trending fault set of the massif and make a 70° angle towards a secondary N000°–030° fault system (Fig. 1).

The Argentera–Mercantour massif and its foreland has been a high relief area since the Early Pliocene (Fauquette *et al.* 1999). Altitudes range between 400 and 3143 m a.s.l. (metres above sea level) (at Mt Gélas) in the gneissic bedrock and 3051 m (at Mt Pelat) in the sedimentary cover (Fig. 1). The combined glacial and river network have deeply eroded and incised the massif, resulting in slope heights of 2000 m. The glaciations history of the area is complex and poorly documented but as in many other Alpine valleys, the morphology of the upper Tinée area was strongly influenced by Rissian and Würmian glacial ages. Most of the current glacial landforms come from the Würmian glaciation. They are characterized by glacial polished surfaces of glacial deposit (Julian 1980). From ^{10}Be dating of polished glacial surface and radiocarbon analysis, Bigot-Cormier *et al.* (2005) and Sanchez *et al.* (2009) reported that the Tinée Valley glacier was totally deglaciated at 12 ka BP whereas higher slope parts were deglaciated around 8 ka BP (Julian 1980). Besides, successive positive pulses since the last main deglaciation have been evidenced in the massif, highlighting a discontinuous deglaciation since the Würm (Julian 1980).

However, glaciers have not been as important as in the other northernmost massifs in the Alps with a southern extension of the ice to a 500 m a.s.l. altitude and a maximum thickness of 500 m in the valley. The summits were also not covered by any ice sheets. As a consequence, in the morphology of the Tinée Valley the mean slope angles vary from 35° up to 1800 m to 25° above this altitude.

Large gravitational deformation inventory

An inventory was established by Jomard (2006) (see also Bois *et al.* 2008). A distinction is made between deformations that are clearly linked to gravity (bounded by a failure surface and a large mobilized volume that correspond to DSL), and deformations that appear diffused in very large volumes of the massif. Such deformations display extensive graben-like features and correspond to large sagging zones of the slopes. Zischinsky (1966) first proposed the term sackung for those surface manifestations of deep-seated rock creeps of foliated bedrocks in the Alps. This kind of movement was then observed in almost all mountain ranges and most authors today use the generic term deep-seated gravitational slope deformation (DSGSD) introduced by Dramis & Sorriso-Valvo (1994) to name the landforms and geomorphic evidence, such as double crested ridges, troughs, antislope scarps and ridge depressions, associated with those deformations (Agliardi *et al.* 2001). The origin of these features (tectonic, gravitational or both) are still poorly understood even if recent

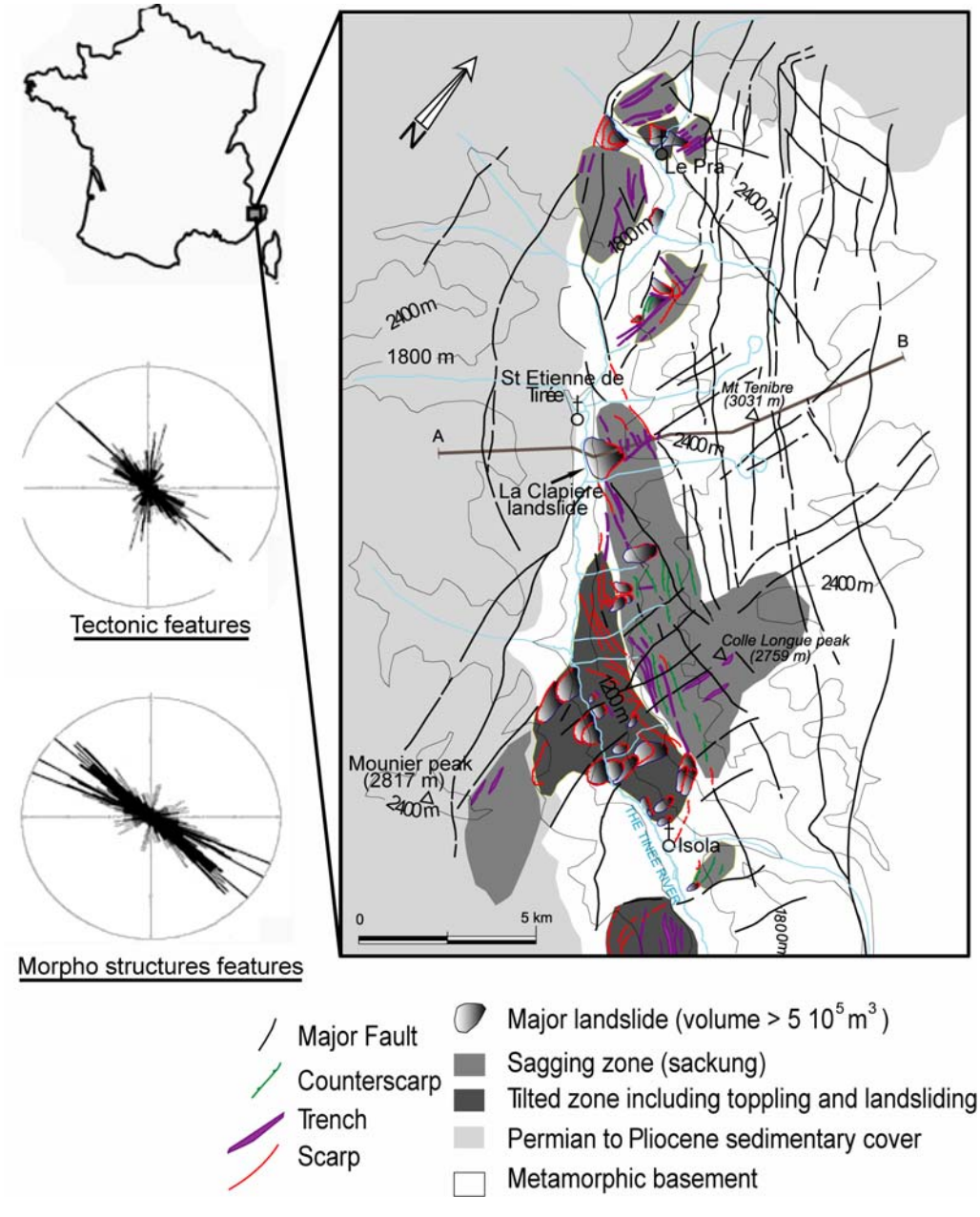

Fig. 1. Major tectonics features and gravitational deformations mapped in the Tinée Valley (modified after Bois *et al.* 2008).

results strongly tend to demonstrate a gravitational origin (Bachmann 2006).

These characteristic morphostuctural features were mapped at the Tinée Valley scale (Jomard 2006). Field investigations within the Tinée slopes showed that most of Würmian glacial morphologies and deposits are affected by gravitational deformations, suggesting gravitational motions since the last deglaciation (Jomard 2006). Most of these observations have been made in the metamorphic basement, in the left bank of the valley. Eight DSGSD zones were recognized containing 20 DSL (Fig. 1).

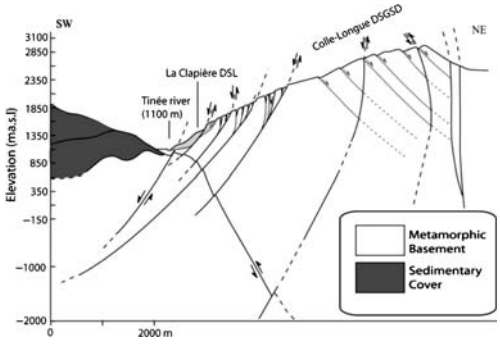

Fig. 2. The La Clapière rockslide embedded in the Colle Longue DSGSD, showing the geometrical relationship between the inherited tectonic structures, DSL and DSGSD (modified after Jomard 2006).

A regional map representing DSGSD and DSL deformations (morphostructures) was compared to the structural map of the massif (Fig. 1).

- The orientations of DSGSD's morphostructures are strongly influenced by both the inherited tectonic framework and the mean N130°-trending foliation. In particular, the major N110°–140°E fault set explains the localization of most of the internal deformations of DSGSD within the valley.
- The other N000°–030°E fault set is also expressed in some cases through deformations secant to the main direction.
- The most developed DSL occurred at the intersection of two fault set, as the La Clapière DSL between the N110°–140°E and N000°–030°E fault set.

The density of morphostructures within DSGSDs appears to be closely dependent on the angular relation between slope direction, foliation and faults orientations. Morphostructures are much more developed when this angle is close to zero. The most developed Colle Longue DSGSD could then be explained by the narrow angle existing between the N140°E main direction of the crests/valley and the N130°E main faults and foliation direction.

The Colle Longue DSGSD represents an area of about 45 km^2. This zone, which presents extensive deformations spreading from the foot to the crests, has been chosen for a more accurate description. Counterscarps are recognized in the upper slope part down to 1800 m a.s.l., although troughs are observed in the lower slope part up to 2100 m a.s.l. Counterscarps can reach 20 m high and always are guided by the foliation planes whose main orientation is N130°–040° NE. It also appears that counterscarps connect at depth to inherited tectonic faults that guide the gravitational deformations. Troughs display 15 m wide apertures that are geometrically associated to downward-dipping (SW) normal and strike-slip fault zones. Both structures affect the slope down to the tributary valleys floor indicating that deformations should be deeper than these valley incisions that can reach 1000 m high. No failure surface enveloping the DSGSD was observed. Compressive features were only observed in some DSL feet encased in the DSGSD zone (like the large active La Clapière DSL). A long-term deformation of the slope is then characterized after the deglaciation. From the chronological point of view, two main observations are made:

- In upper slope parts (>1800 m), gravitational deformations affect Würmian glacial morphologies of high-altitude tributary glaciers, rock glaciers and active screes. Glacial sediments filling cracks are also observed in a number of counterscarps. Deformations are mostly represented by counterscarps and scarps.
- In lower slope parts, deformations affecting Würmian deposits and morphologies are represented by scarps. Troughs are filled with colluviums and no glacial sedimentary fillings are observed.

On the La Clapière slope (Jomard 2006), a trough located on a down-slope normal fault was detailed (Fig. 3). The fault, characterized by its gouge and slickenslide planes, was recently toppled and created a large tension aperture (10 m) infilled by regular post-glacial colluviums sedimentation. The toppling of rock columns allowed an intense fracturing of the downward wall of the fault. Finally, this intense fracturing gives the possibility for sliding surfaces to develop and cross-cut the overall structure (Fig. 3).

Chronological constraints based on ^{10}Be dating of gravitational scarps, troughs and landslide surfaces in the Tinée area show three successive periods of gravitational instabilities (Bigot-Cormier *et al.* 2005; Sanchez *et al.* 2009). The first closely post-dates the last deglaciation event (12–13 ka) with an age of 10–11 ka, a second destabilization occurs at 7–9 ka BP and a third at 2.5–5.5 ka BP. Thus, gravitational slope deformations have been effective at least since 12 ka BP, leading to the present active large deep-seated landslides such as La Clapière.

Slope-scale analysis of La Clapière

Field analysis

The La Clapière slope (Fig. 2) is one of the most active DSLs of the valley. This DSL affects 60×10^6 m^3 of rock of the metamorphic basement.

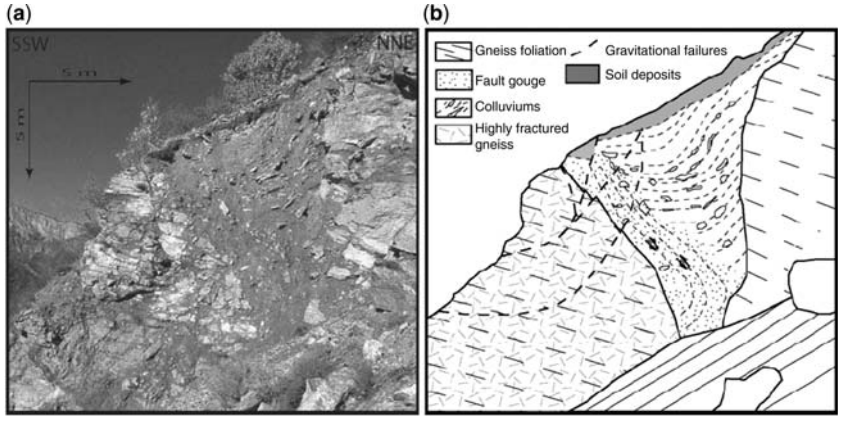

Fig. 3. Trough cross-section (modified after Jomard 2006). Tilted normal fault gouge infilled with post-glacial colluvium affected by recent failure. (**a**) Photograph and (**b**) interpretation.

The first activity reported dates from the early 1930s, with a peak evolution between 1960 and 1990 leading to a 130 m-high scarp development in the middle of the slope. Thus, since the 1990s, structural investigations (Follacci 1987; Ivaldi 1991), geomechanicals triaxial experiments on rock samples, hydrogeological studies (Cappa *et al.* 2004; Guglielmi *et al.* 2005), numerical modelling and geophysical surveys (Lebourg *et al.* 2005; Jomard *et al.* 2007, 2010) have been performed underlining a complex post-failure behaviour. The La Clapière DSL is geometrically bound by N110°–140°E and N010°–030°E fault sets (Fig. 1). Other morphological signs of gravitational destabilization are guided by those tectonic orientations, and are represented inside and outside the DSL boundaries, mainly consisting of troughs aligned on tectonic fault scarps (Fig. 3). These troughs show, respectively, a trace linear far from the active DSL, curved close to the DSL and dislocated within the landslide body. Fifteen troughs were mapped with an average N120° direction and a 100–5000 m length (Fig. 4) that indicated a deep slope deformation in agreement with the observations made in the valleys bounding the slope (Fig. 2).

Troughs were mainly observed from the toe to the middle of the slope (1500–2100 m in elevation) and their evolution is clearly linked to the initiation of the La Clapière DSL. Their average orientation is parallel to the slope, although troughs closed to the western boundary of the currently active DSL have an orientation close to N130° (Fig. 4). Troughs 1–4 that are the closest to the active DSL scarp are highly deformed (and even cut by the scarp) while torsion progressively vanishes from troughs 5–15. Troughs 1, 6 and 14, and the west lateral scarp propagation of La Clapière active DSL, were dated using an *in situ* produced ^{10}Be cosmogenic approach (Bigot-Cormier *et al.* 2005; Sanchez *et al.* 2009). The result suggest that the troughs become progressively younger from trench 1 (10 ka BP), 6 (7.2 ka BP) to 14 (5.6 ka BP), meaning that a deformation of the slope propagated from the toe to the top of the slope at about 4.4 ka BP.

The upper lateral scarp of the currently active DSL was dated at 3.6 ka BP, showing that after the up-slope deformation propagation a deep failure initiated in the middle part of the slope that ultimately bounds the currently active DSL.

Two-dimensional (2D) physical modelling experiments were performed reproducing a NNE–SSW cross-section of the La Clapière slope in order to analyse the links between superficial and deep-seated deformations (Figs 5 & 6).

Two-dimensional physical modelling of the 'La Clapière' slope

A complete description of the analogue material (called *Slope*1) and the loading device developed to perform our scaled physical models is available in Bachmann *et al.* (2004), Chemenda *et al.* (2005) and in Bois *et al.* (2008). A short description is available in the Appendix of this paper. For these models a scaling factor of 1/50 000 was chosen. The vertical faults have been numbered from F1 near the valley toe to F6 near the crest. Two distinct configurations of the slope were tested:

- a homogenous model (Fig. 5) that must be considered as a massive homogeneously fractured massif without any major localized weak zone;

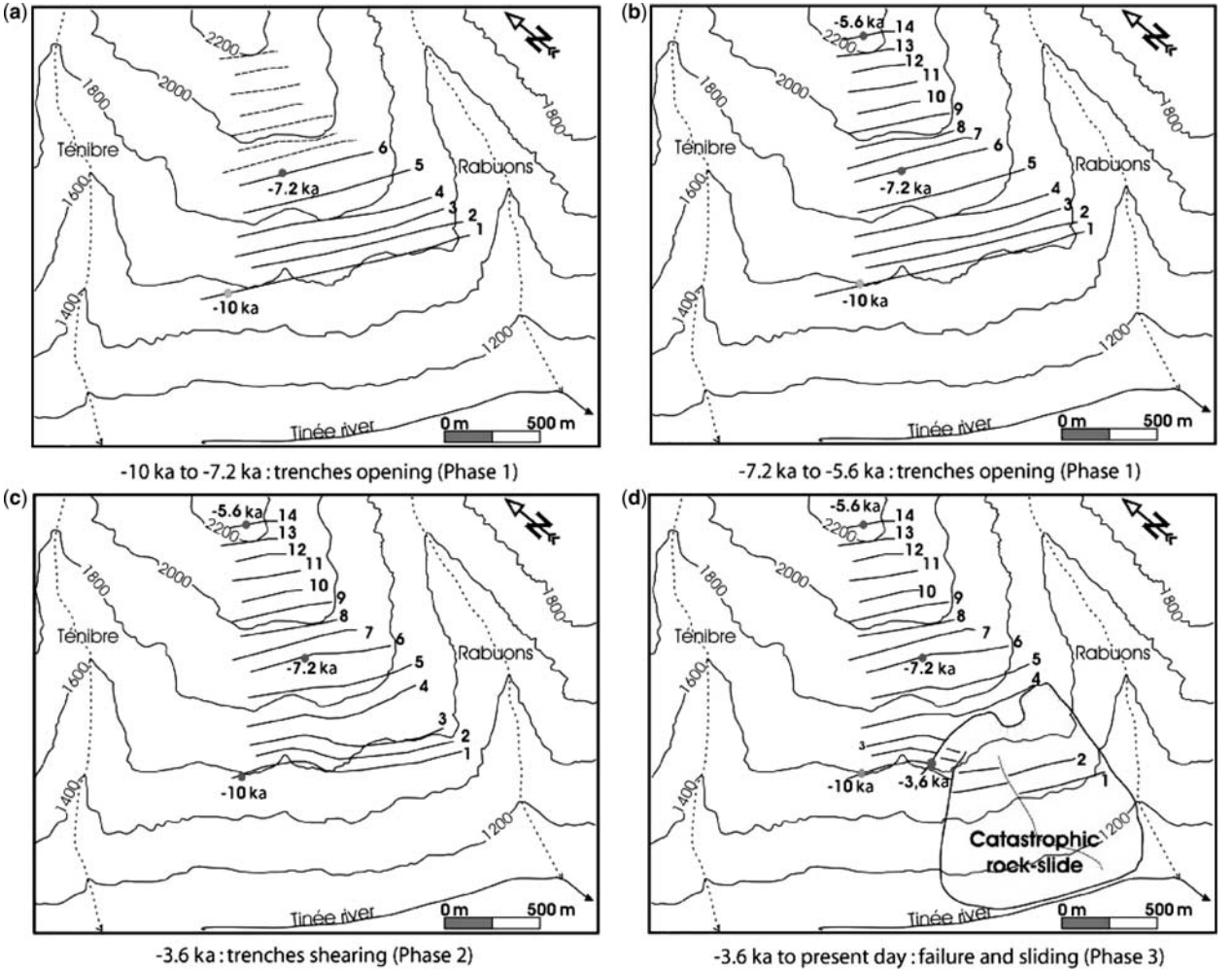

Fig. 4. Evolution of the La Clapière slope deformation for the last 10 ka BP. (**a**) and (**b**) Troughs opening from 1600 to 2250 m elevation a.s.l.; (**c**) surface shearing close to the future rockslide area; (**d**) rockslide collapse and sliding (modified after El Bedoui *et al.* 2009).

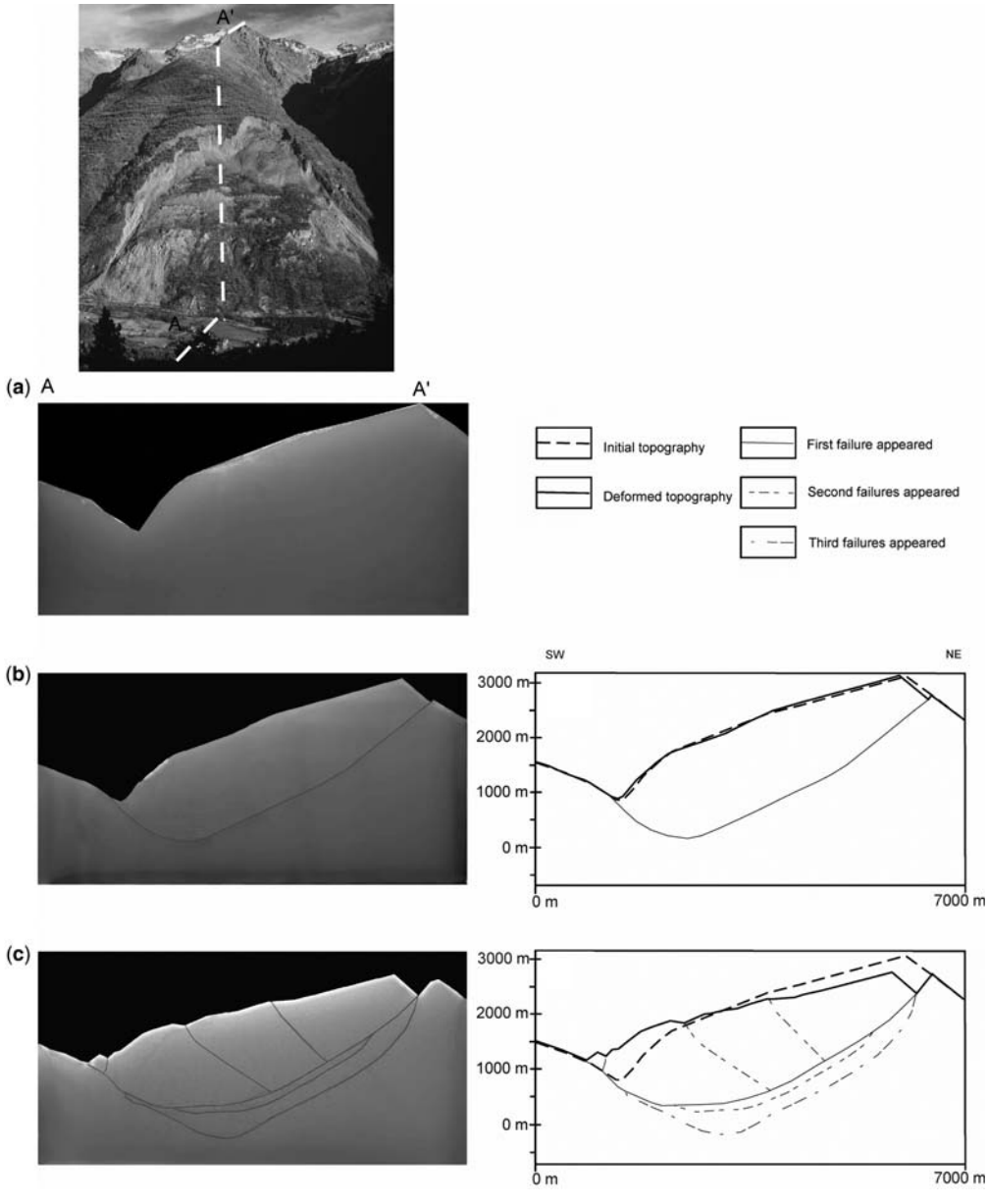

Fig. 5. Homogeneous model of the La Clapière slope: (**a**) the non-deformed model; (**b**) the first deformation stage and its interpretative sketch; and (**c**) the last deformation stage and its interpretative sketch (modified after Bois *et al.* 2008).

- a model considering the N140° fault zones previously presented (Fig. 6). The listric geometry of those faults was deduced from field investigations (Fig. 2).

Homogeneous model. On the initial deformation stage (Fig. 5b), a deep sliding surface was formed inside the model.

Its maximum depth was equivalent to 1500 m. This sliding surface bounded a large unstable volume involving the entire massif. A 100 m- high scarp was formed behind the topographic crest.

On the final deformation stage, the sliding surface becomes a more complex fracture network. Its width increased with the displacement of the

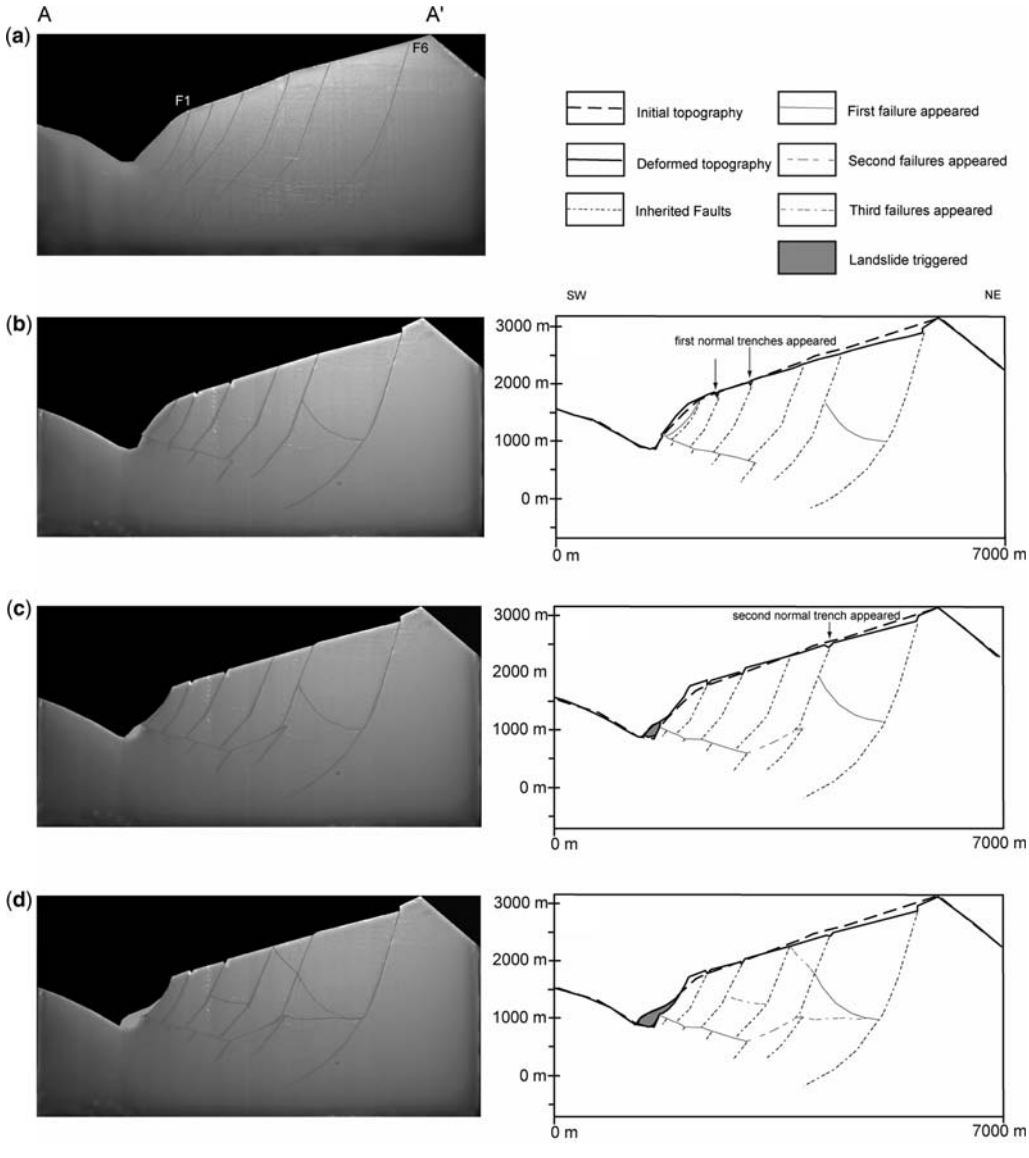

Fig. 6. A slope model of La Clapière cut by six inherited normal listric faults: (**a**) the non-deformed model; (**b**) the first deformation stage and its interpretative sketch; (**c**) the second deformation stage and its interpretative sketch; and (**d**) the last deformation stage and its interpretative sketch (modified after Bois *et al.* 2008).

sliding unit (Fig. 5c). This complex failure zone reached a maximum depth of 2200 m and was associated with two antithetic newly formed faults. The escarpment located behind the topographic crest kept growing to reach a maximum of 400 m.

A slope cut by six inherited normal listric faults. During the initial deformation stage (Fig. 6a), most of the superficial non-elastic deformation was localized on three inherited normal faults and on a newly formed gravitational fault. On the inherited fault close to the topographic crest (F6) a 100 m-high escarpment appeared (Fig. 6b). On the inherited faults close to the slope toe (F2 and F3) two troughs appeared (Fig. 6b).

Finally, a newly formed gravitational fault formed at the slope toe that propagated inside the massif rather like a subhorizontal thrust fault

(Fig. 6b). Internal irreversible deformations took place along this newly formed thrust fault and also along an antithetic normal fault initiating from the inflection point of fault F6 towards the topographic surface (Fig. 6).

During the second deformation stage, the deformation increased (Fig. 6c): another normal trench appeared at the top of the fault F5. The newly formed thrust fault propagated inside the model and a relatively small superficial DSL was finally triggered between the first normal fault and the slope toe.

In the last deformation stage (Fig. 6d), the sliding surface propagated inside the model through the connection of the inflection points of faults F4–F6, delimiting a deep gravitational moving zone. The first antithetic fault propagated and reached the topographic surface. The hillside was affected by a second DSL, which was a retrogressive one.

The fractured model deformation can then be summarized as follows.

- The normal troughs are formed on the faults close to the valley immediately followed by the appearance of the first normal shifting on faults close to the topographic crest.
- The first antithetic faults are formed, and a sliding surface (i.e. thrust fault) propagates from the toe.
- New troughs are created higher on the slope due to a retrogressive deformation process. The sliding surface propagates and a small-scale DSL is triggered.
- The sliding surface is connected to the F6 fault delimiting the total moving mass. The deformation of this part of the slope leads to the formation of successive landslides that affect the slope.

Modelling major results. On one hand, the deformation pattern obtained in the homogeneous configuration showed that even if the kinematics of the rupture is coherent, the localization of the deformation is not evident. Indeed, it seems obvious that the 'La Clapière' slope cannot be considered to have fractured homogeneously. Some localized weak zones have to be taken into account, such as the N140° faults zones. This is confirmed by the second model configuration for which it appears clearly that the deformation is mainly localized on pre-existing faults.

However, on the other hand, those models are 2D models developed according to a NNE–SSW cross-section of the 'La Clapière' slope, and owing to this simplification some structures have not been considered (e.g. other inherited faults such as the N030° ones). It is reasonable to say that those structures must also have had an influence on the localization of the deformation and, at a larger scale, on the global deformation pattern of the massif.

From DSGSD to catastrophic failure at the slope scale

Based on field investigations and absolute ages (^{10}Be), El Bedoui *et al*. (2009) calibrated a model of the slope evolution for the last 10 ka. Physical modelling shows a very good agreement with this proposed model based on field and dating work underlining the link between those superficial deformations and the failure propagation at depth.

From 10 to 5.6 ka BP (Fig. 4) extensional structures (troughs) spread from the toe to the top of the slope, showing a good correspondence with physical modelling (Fig. 6b, c) (phase I). The trench-like morphology is explained by the reactivation of inherited structures that could have been induced by the stress release effects in the slope related to glacial retreat of the last glaciation. This phase I could be related to the deep fracture retrogressive propagation showed by physical modelling (Fig. 6c, d).

From 5 to 3.6 ka BP (Fig. 4) a shearing of troughs occurred in the western lower part of the slope that also displayed a high vertical displacement (phase II). This 3D twisting of surface troughs, which is related to shear deformations developing deep in the slope, could be induced by preferential tangential movements along a major N030° reactivated vertical fault zone located in the east part of the slope.

At 3.6 ka BP (Fig. 4) a failure initiates, wrapping this eastern lower part of the slope. In the last 50 years this failure evolved in a large-scale failure surface bounding the currently active La Clapière DSL (phase III).

^{10}Be ages indicate that phase I (troughs opening – DSGSD) propagates over a very long period (6 ka BP). Phase II (troughs shearing) is only constrained by two dated events: the trench opening (10 ka BP) and the first failure associated with the rockslide (3.6 ka BP).

If physical modelling does not allow a kinematic model of the slope evolution, results underline the fact that the first rockslide event was synchronous with the upper and younger trench (dated at 5.2 ka BP). It could indicate that the trench shearing more probably occurred between 5.2 and 3.6 ka BP rather than immediately after the trench opening at 10 ka BP. The kinematics of slope deformation have been characterized in two dimensions and extended in three dimensions, and suggest a non-linear creep-like phenomenon. The significance of the deduced model needs to be discussed in a mechanical way and compared to other places in the valley to assess its validity.

Discussion

Mechanical processes at the slope scale

Rock slope failure in general results from many different processes and among these the influences of the pre-existing heterogeneities (such as bedding planes, foliation and fault zones) (Terzaghi 1962; Kato & Hada 1980; Chigira 1985; Agliardi *et al.* 2001) the mountain height and slope gradient appear to be predominant. Rock slope stability is thus highly dependent on the specific characteristics of the fault zones (e.g. density of the fault network, persistence at depth, the geometry of the faults, etc.) (Hermanns & Strecker 1999). Our study underlines the major role played by regional scale weak planes that correspond to inherited major fault zones (Bois *et al.* 2008).

The temporal evolution of slope deformation at La Clapière is in good accordance with laboratory experiments that display highly non-linear creep-like phenomena even for hard rocks. In previous work conducted on the gravitational evolution of rock slopes (Brückl & Parotidis 2005; Petley *et al.* 2005; Apuani *et al.* 2007) the evolution from DSGSD to a localized catastrophic failure is physically and mechanically regarded as a creep-like phenomenon. Brückl & Parotidis (2005) numerically studied the slope instabilities resulting from deep-seated gravitational creep and the transition from a slow evolution phase to rapid sliding. The process of subcritical growth was considered to explain the primary phase of deep-seated gravitational creep because it allowed the progressive damage of the rock mass at a lower stress than the rock strength. It could correspond to the progressive failure growth at depth characterized by troughs opening and twisting at the surface. The total failure at depth then outlines the currently active rockslide, acceleration of the movements being related to the 'smoothing of the basal surface'.

Another first-order process that has an influence on strength reduction, and thus on damage process, is weathering controlled by climatic and fluids circulations (Hill & Rosenbaum 1998; Hall & André 2001; Pellegrino & Prestininzi 2007). It also has a strong control on the failure process, especially in the case of granitic rocks in the Alps (Girod 1999; Jaboyedoff *et al.* 2004). Indeed, the alteration of such rocks has two main influences: on the one hand, it leads to the formation of clays; thus reducing the fluid circulation and increasing the pressure (Girod 1999). This is particularly true in faulted zones where alteration is concentrated basically along localized weak zones: fractures and faults (Migon & Lidmar-Bergström 2002; Wyns 2002). On the other hand, weathering causes a progressive strength reduction of the rock material, which is stress dependent. This softening is generally maximal at the surface and diminishes with depth (Chigira 2001).

Even if this contributing factor has not been taken into account by the physical models, Chemenda *et al.* (2009) used a 2D finite-element numerical model to show that, in the case of the La Clapière slope, a progressive reduction in the mechanical resistance (due to a progressive reduction in the model cohesion), combined with the particular geometry of glacial Alpine valleys, can lead to the DSL.

A time-dependent model (Fig. 7) calibrated on the La Clapière slope failure was proposed in order to fit the observed surface displacements as function of time (El Bedoui *et al.* 2009). This model presents three phases: (1) very slow displacements over a long time period (several mm year^{-1}); (2) an increase in surface displacements related to a deep slide plane (crack coalescence); and (3) a catastrophic evolution over a very short time period.

Extrapolation of the model at the valley scale

The La Clapière slope is part of the Colle Longue DSGSD. Looking at the Tinée Valley scale, different evolution stages were observed, from pre-failure stages characterized by troughs dislocation, to active and fossil DSL. Two representative localities were studied: the Isola slope and the Pra slope (Figs 1 & 8).

The Isola slope is located downstream of the upper Tinée Valley. This slope is also embedded in the Colle Longue DSGSD (Figs 1 & 8). The average slope is 35° in the basal part (from 850 to 1700 m elevation) and 25° in the upper part. A large series of N120° troughs crop out in the basal part, extending laterally over distances of 500 m. A surface shearing of these troughs was located at elevations of between 1000 and 1500 m, which is similar to the La Clapière case and indicates a contrast of surface velocities between the upper stable part of the slope and the lower more intensely deformed area. The lower slope part shows signs of shearing that are as developed as those on the La Clapière slope (Fig. 8). It indicates that this slope can correspond to the second stage of the evolution model of slope deformation (Figs 6 & 7). This advanced stage of slope deformation is further exacerbated by very active rockfall activity and may indicate a future landsliding activity during the next century.

Conclusion

Coupling the different approaches presented in this paper has allowed the elaboration of a 4D evolution

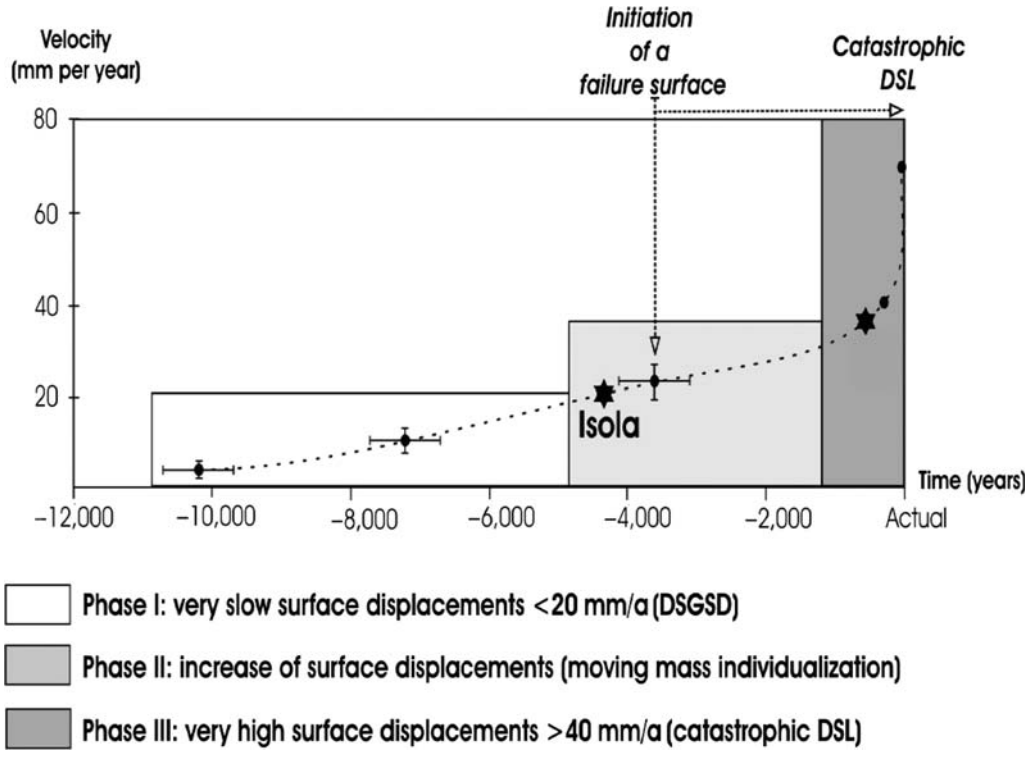

Fig. 7. Curve of time-dependent progressive failure calibrated on the La Clapière slope (modified after El Bedoui *et al.* 2009).

model of rock slope destabilization linking failure propagation at depth and subsequent deformations at the surface. The model seems to be well constrained for the La Clapière slope and seems also to be valid at the Tinée Valley scale. Furthermore, as the spatial correlation between gravitational deformation and weakened zones of inherited faults suggest, the major structural framework has a key role in such processes. Thus, by comparison with other slopes, we suggest that kinematics of slope evolution are controlled by a critical spacing/arrangement of major inherited faults. De facto, the deglaciation and the consecutive slope angle increase of the valley is supposed to have a strong influence on slope destabilization due to modifications of *in situ* stress condition and rock strength parameters.

The main implication of these results is that the model proposed based on the La Clapière slope can be considered as a reference at the valley scale and, probably more widely, at the massif scale as proposed by Jomard (2006). Large-scale geomorphological studies (Jomard 2006) should be coupled with instrumental surveys (GPS) performed at the valley scale and mechanically scaled models; this will, respectively, allow: (i) an estimation of volumes potentially mobilized during the destabilization (based on deformation of morphological signs; i.e. troughs); and (ii) a rough estimation of time prior to failure by comparison between instrumental velocities and the reference calibrated on the La Clapière slope.

Authors sincerely express their gratitude to the GIS CURARE who financed this project and to the reviewers for their useful remarks.

Appendix

*Slope*1 is a low frictional elasto-brittle–plastic analogue material with strain softening (Chemenda *et al.* 2005). This material represents a compositional system based on liquid and solid hydrocarbons. To create a model, the melted analogue material *Slope*1 is moulded into a rigid box at a temperature of 50 °C. In order to create the faults a series of openings cut in the two opposite lateral sides of the model box are used to position taut strings.

After cooling to a temperature of 20 °C, at which the crystallized material is strong enough to be easily

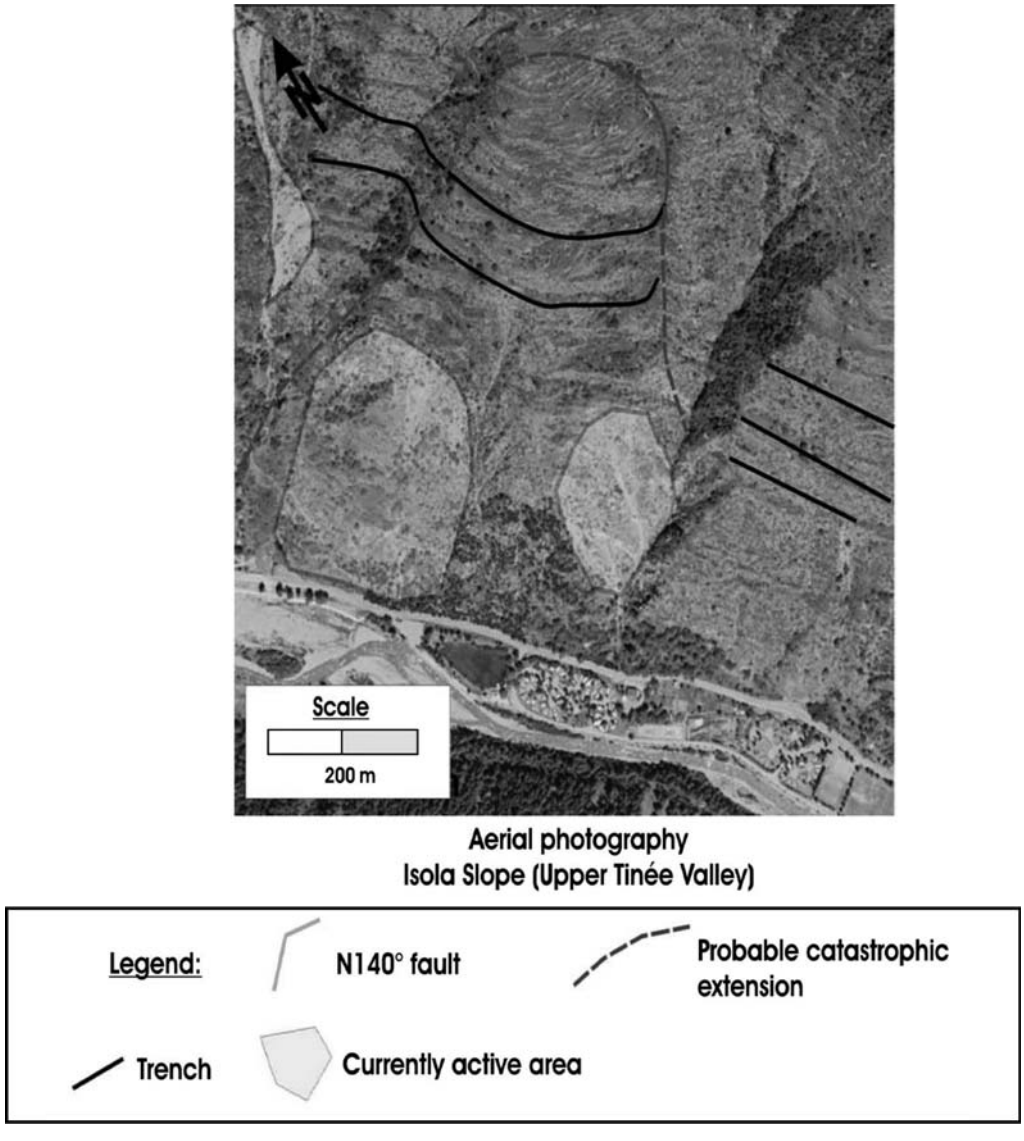

Fig. 8. Morphostructures of the Isola slope.

handled without damage and easily cut with the strings without being damaged in areas other than the cuts, strings are translated along the slots to generate the faults and then removed. The model surface was then shaped to the desired topography (Figs 5a & 6a). The length of the model is thus equal to 14 cm and the width (third dimension) is equal to 30 cm. The third dimension has been chosen large enough to prevent any edge effects.

Once the model is prepared it is loaded into a vertical accelerator table. The latter consists of a mobile platform that can be lifted up to 2 m and then released. During its free fall the model reaches a maximum velocity of 6 m s^{-1}. The platform is then rapidly but smoothly decelerated to zero velocity when it comes into contact with a progressive shock absorber of 5 cm stroke. During this phase the model undergoes a strong vertical deceleration (up to 500 m s^{-2}). This deceleration acting in the same direction as gravity is repeated until failure develops, usually at approximately 100 cycles. Preliminary calibration tests are needed to determine which acceleration must be imposed onto a model for a given configuration (geometry, prefracturing state, etc.) in order to observe

failure for a number of loading cycles ranging from 100 and 150.

Model deformation can be observed accurately after each acceleration cycle. This discrete loading technique has proved to be equivalent to a continuous quasi-static loading (Chemenda *et al.* 2005).

The main similarity criterion is:

$$\frac{\sigma_c^o}{\rho^o g^o H^o} = \frac{\sigma_c^m}{\rho^m g^m H^m} \quad (1)$$

where ρ is density and g is gravity acceleration, σ_c is the strength under uniaxial compression and H is the spatial scale of the phenomenon (the mountain height H, for example). The superscripts 'o' and 'm' mean original and model, respectively.

To ensure that the deformation will be localized along brittle structures, as in nature, *Slope*1 has to exhibit a high degree of softening. Hence, the experiments were carried out at a fixed temperature of 20 °C. This mechanical behaviour is comparable to the strength degradation behaviour introduced into some numerical models. At this temperature the coefficient of friction measured on the pre-existing fractures is $\mu = 0.2$.

Cross-sections were made at the end of each experiment by cutting the model at various positions after cooling it to 10 °C in order to increase its strengths. Some experiments were stopped in the early stages of model deformation to analyse the corresponding evolution of internal slope deformation.

References

Agliardi, F., Crosta, G. & Zanchi, A. 2001. Structural constraints on deep-seated slope deformation kinematics. *Engineering Geology*, **59**, 83–102.

Apuani, T., Masetti, M. & Rossi, M. 2007. Stress–strain–time numerical modelling of a deep-seated gravitational slope deformation: preliminary results. *Quaternary International*, 171–172, 80–89.

Augustinus, P. C. 1995. Glacial valley cross-profile development: the influence of in situ rock stress and rock mass strength, with examples from the Southern Alps, New Zealand. *Geomorphology*, **14**, 87–97.

Bachmann, D. 2006. *Modélisation physique tridimensionnelle des mouvements gravitaires de grande ampleur en milieu rocheux*. PhD thesis, Université de Nice Sophia Antipolis, Nice, France.

Bachmann, D., Bouissou, S. & Chemanda, A. 2004. Influence of weathering and pre existing large scale fractures on gravitational slope failure: insights from 3-D physical modelling. *Natural Hazards and Earth System Sciences*, **4**, 711–717.

Ballantyne, C.-K. 2002. Paraglacial geomorphology. *Quaternary Science Reviews*, **21**, 1935–2017.

Bigot-Cormier, F., Braucher, R., Bourlès, D., Guglielmi, Y., Dubar, M. & Stéphan, J. F. 2005. Chronological constraints on processes leading to large active landslides. *Earth and Planetary Science Letters*, **235**, 141–150.

Bois, T., Bouissou, S. & Guglielmi, Y. 2008. Influence of major inherited faults zones on gravitational slope deformations: A two-dimensional physical modelling of the La Clapière area (Southern French Alps). *Earth and Planetary Science Letters*, **272**, 709–719; doi: 10.1016/j-epsl_2008.06.006.

Brideau, M.-A., Stead, D., Kinakin, D. & Fecova, K. 2005. Influence of tectonic structures on the Hope Slide, British Columbia, Canada, *Engineereing Geology*, **80**, 242–529.

Brückl, E. & Parotidis, M. 2005. Prediction of slope instabilities due to deep-seated gravitational creep. *Natural Hazards and Earth System Sciences*, **5**, 155–172.

Cappa, F., Guglielmi, Y., Soukatchoff, V. M., Mudry, J., Bertrand, C. & Charmoille, A. 2004. Hydromechanical modelling of a large moving rock slope inferred from slope levelling coupled to spring long-term hydrochemical monitoring: example of the La Clapière landslide (Southern Alps, France). *Journal of Hydrology*, **291**, 67–90.

Chemenda, A., Bois, T. & Bouissou, S. 2009. Numerical modeling of the gravity-induced destabilization of a slope: example of the Clapière landslide, southern France. *Geomorphology*, **109**, 86–93; doi: 10.1016/j.geomorph.2009.02.025.

Chemenda, A., Bouissou, S. & Bachmann, D. 2005. Three dimensional physical Modeling of Deep-Seated Landslides: new technique and first results. *Journal of Geophysical Research*, **110**, F04004; doi: 10.1029/2004JF000264.

Chigira, M. 1985. Mass rock creep of crystalline schist: minor structures formed by mass rock creep. *Journal of Japanese Society of Engineering Geology*, **26**, 25–79.

Chigira, M. 2001. Micro-sheeting of granite and its relationship with landsliding specially after the heavy rainstorm in June 1999, Hiroshima prefecture, Japan. *Engineering Geology*, **29**, 219–231.

Corsini, M., Ruffet, G. & Caby, R. 2004. Alpine and late Hercynian geomorphological constraints in the Argentera massif (Western Alps). *Eclogae Geologicae Helvetiae*, **97**, 3–15.

Dramis, F. & Sorriso-Valvo, M. 1994. Deep-seated gravitational slope deformations, related landslides and tectonics. *Engineering Geology*, **38**, 231–243.

El Bedoui, S., Guglielmi, Y., Lebourg, T. & Pérez, J. L. 2009. Deep-seated failure propagation in a fractured rock slope over 10 000 years: the La Clapière slope, the south-eastern French Alps. *Geomorphology*, **105**, 232–238; doi: 10.1016/j.geomorph.2008.09.025.

Evans, S. G. & Clague, J. J. 1994. Recent climatic change and catastrophic geomorphic processes in mountain environments. *Geomorphology*, **10**, 107–128.

Fauquette, S., Suc, J.-P. *et al.* 1999. Climate and biomes in the west Mediterranean during the Pliocene. *Palaeogeography, Palaeoclimatology, Palaeoecology*, **152**, 15–36.

Faure-Muret, A. 1955. *Etudes géologiques sur le massif de l'Argentera-Mercantour et ses enveloppes sédimentaires*. Mémoire de la Carte Géologique de France.

Ferrara, G. & Malaroda, M. 1969. Radiometric age of granitic rocks from the Argentera massif (MAritime Alps). *Bollettino della Società Geologica Italiana*, **88**, 311–320.

Follacci, J. P. 1987. Les mouvements du versant de la Clapière à Saint Etienne de Tinée (Alpes Maritimes). *Bulletin de Liaison des Ponts et Chaussées*, **150/151**, 39–54.

Girod, F. 1999. *Altération météorique de roche granitique en milieu alpin: le cas de l'orthogneiss associé à l'éboulement de Randa (Mattertal, Valais, Suisse)*. PhD thesis, Université de Lausanne.

Guglielmi, Y., Cappa, F. & Binet, S. 2005. Coupling between hydrogeology and deformation of montainous rock slopes: insights from La Clapière area (southearn Alps, France). *Comptes rendus Géosciences*, **337**, 1154–1163.

Hall, K. & André, M. F. 2001. New insights into rock weathering from high-frequency rock temperature data: an Antarctic study of weathering by thermal stress. *Geomorphology*, **41**, 23–35.

Hermanns, R. L. & Strecker, M. R. 1999. Structural and lithological controls on large Quaternary rock avalanches (sturzstroms) in arid northwestern Argentina. *Geological Society of America*, **111**, 934–948.

Hill, S. E. & Rosenbaum, M. S. 1998. Assessing the significant factors in a rock weathering system. *Quarternary Journal of Engineering Geology and Hydrology*, **31**, 85–94.

Hippolyte, J.-C., Brocard, G. *et al.* 2006. The recent fault scarps of the Western Alps (France): tectonic surface ruptures of gravitational sackung scarps? A combined mapping, geomorphic, levelling, and ^{10}Be dating approach. *Tectonophysics*, **418**, 255–276.

Hutchinson, J. N. 1988. General Report: morphological and geotechnical parameters of landslides in relatio to geology and hydrogeology. *Proceedings of the 5th International Symposium on Landslides*, Lausanne, 3–35.

Ivaldi, J. P., Guardia, P., Follacci, J. P. & Terramorsi, S. 1991. Plis de couverture en échelons et failles de second ordre associés à un décrochement dextre de socle sur le bord nord-ouest de l'Argentera (Alpes-Maritimes, France). *Compte Rendus de L'Academie des Sciences, Paris*, **313**, 361–368.

Jaboyedoff, M., Baillifard, F., Bardou, E. & Girod, F. 2004. Weathering, cycles of saturation-unsaturation, and strain effects as principal processes for rock mass destabilization. *Quarterly Journal of Engineering Geology and Hydrogeology*, **37**, 95–103.

Jarman, D. 2006. Large rock slope failures in the Highlands of Scotland: characterisation, causes and spatial distribution. *Engineering Geology*, **83**, 161–182.

Jomard, H. 2006. *Analyse multi-échelles des déformations gravitaires du Massif de l'Argentera Mercantour*. PhD thesis, Nice Sophia-Antipolis University.

Jomard, H., Lebourg, T., Guglielmi, Y. & Tric, E. 2010. Electrical imaging of sliding geometry and fluids associated with a deep seated landslide (La Clapière, France). *Earth Surface Processes and Landforms*, **35**, 588–599.

Jomard, H., Lebourg, T. & Tric, E. 2007. Identification of the gravitational boundary in weathered gneiss by geophysical survey: La Clapière landslide (France). *Journal of Applied Geophysics*, **62**, 47–57.

Julian, M. 1980. *Les Alpes Maritimes Franco-Italiennes. Etude Géomorphologique*. PhD thesis, Aix-Marseille II University, Marseille.

Julian, M. & Anthony, E. 1996. Aspect of landslide activity in the Mercantour Massif and the French Riviera, southeastern France. *Geomorphology*, **15**, 275–289.

Kaneko, K., Otani, K. J., Noguchi, Y. & Togashiki, N. 1997. Rock fracture mechanics analysis of slope failure. Deformation and Progressive Failure. *In*: Asaoka, A., Adachi, T. & Oka, F. (eds) *Geomechanics*. Elsevier, New York, 671–676.

Kato, J. & Hada, S. 1980. Landslides of the Yoshino–Gawa water system and its geological aspects. Research Reports of the Kochi University. *Natural Science*, **28**, 127–140.

Lebourg, T., Binet, S., Tric, E., Jomard, H. & El Bedoui, S. 2005. Geophysical survey to estimate the 3D sliding surface and the 4D evolution of the water pressure on part of a deep seated landslide. *Terra Nova*, **17**, 399–406.

Migon, P. & Lidmar-Bergström, K. 2002. Europe: problems of dating and interpretation of geological records. *Catena*, **49**, 25–40.

Pellegrino, A. & Prestininzi, A. 2007. Impact of weathering on the geomechanical properties of rocks along thermal-metamorphic contact belts and morphoevolutionary. *Geomorphology*, **87**, 176–195.

Petley, D. N., Mantovani, F., Bulmer, M. H. & Zannoni, A. 2005. The use of surface monitoring data for the interpretation of landslide movement patterns. *Geomorphology*, **66**, 133–147.

Sanchez, G., Rolland, Y., Corsini, M., Braucher, R., Bourles, D., Arnold, M. & Aumaître, G. 2009. Relationships between tectonics, slope instability and climate change: cosmic ray exposure dating of active faults, landslides and glacial surfaces in the SW Alps. *Geomorphology*, **117**, 1–13; doi: 10.1016/j.geomorph.2009.10.019.

Sartori, M., Baillifard, F., Jaboyedoff, M. & Rouiller, J. D. 2003. Kinematics of the 1991 Randa rockslides (Valais, Switzerland). *Natural Hazards and Earth System Sciences*, **3**, 423–433.

Savage, W. Z. & Varnes, D. J. 1987. Mechanics of gravitational spreading of steep-sided ridges (sackung). *Bulletin of Engineering Geology and the Environment*, **35**, 31–36.

Scavia, C. 1995. A method for the study of crack propagation in rock structures. *Géotechnique*, **45**, 447–463.

Terzaghi, K. 1962. Stability of steep slopes in hard unweathered rock. *Géotechnique*, **12**, 251–270.

Tibaldi, A., Rovida, A. & Corazzato, C. 2004. A giant deep-seated slope deformaion in the Italian Alps studied by paleoseismological and morphometric techniques. *Geomorphology*, **58**, 27–47.

Tricart, P. 1984. From passive margin to continental collision; a tectonic scenario for the western Alps. *American Journal of Sciences*, **284**, 97–120.

WILLENBERG, H. 2004. *Geologic and kinematic model of a complex landslide in crystalline rock (Randa, Switzerland)*, PhD thesis, Swiss Federal Institute of Technology Zurich.

WYNS, R. 2002. Climat, eustatisme, tectonique: quels contrôles pour l'altération continentale? Exemple des séquences d'altération cénozoïques en France. *Bulletin d'Information Géologie des Bassins, Paris*, **39**, 5–16.

ZISCHINSKY, U. 1966. On the deformation of high slopes. *In*: *Proceedings of the First International Conference of the International Society of Rock Mechanics, Lisbon*, Volume 2. International Society of Rock Mechanics, Lisbon, 179–185.